SCA2003-49: SENSITIVITY STUDIES OF FLUID FLOW ACROSS WATER-SATURATED FAULTS WITH HIGH ENTRY PRESSURE

M.T. Tweheyo, E. Knudsen, and O. Torsæter (Norwegian University of Science & Technology, Trondheim, Norway); J.K. Ringen (STATOIL, Stavanger, Norway)

This paper was prepared for presentation at the International Symposium of the Society of Core Analysts held in Pau, France, 21-24 September 2003

ABSTRACT

Water-saturated faults with high oil entry pressure and very low permeability may hinder the flow of hydrocarbons in reservoirs due to formation of traps or fault-related compartments. This compartmentalisation can lead to lower than expected reservoir performance as has been observed in several oilfields in the Brent Province in the North Sea. This paper presents numerical simulations (using an Eclipse Simulator) of two-phase (oil/water) flow in models that mimic reservoir/fault situations. The fault rock is initially 100% water saturated and is expected to continue acting as a sealing fault/barrier to oil flow until its capillary entry pressure for oil is exceeded.

A ceramic material has been selected to represent the fault while the reservoir zone is Berea sandstone - both rocks were characterised by special core analyses. The ceramic material can be viewed as a porous membrane across which transport is obtained by a potential difference, which was achieved by pressure drawdown due to production. Relative permeability and capillary pressure data were derived from established correlations and mercury porosimetry data. The results show that fluid conductivity in the fault varies with initial water saturation in the reservoir zone. Also, the oil breakthrough and recovery are highly controlled by the fault properties (permeability, entry pressure and thickness).

INTRODUCTION

The interaction between faults and oil production in hydrocarbon reservoirs is a subject that needs more understanding and attention. Although the subject has been under discussion for some time, it is recently that improvements in technology have enabled mapping of fault distributions and allowed study of their consequences to fluid flow [1,2]. Such technical advances have been in borehole and seismic imaging and have helped mapping of faults and fracture distribution in reservoirs, but the complexity of fault systems and heterogeneity has shown that different faults affect fluid flow in different ways.

Faults can form traps that keep hydrocarbons in place or they can hinder flow by forming compartments. In the Brent Province for example, compartmentalised oilfields have been identified and their reservoir performance have shown that such fault distribution can lead to lower than expected recoveries [3]. However, other fault systems have been found to act as conduits that facilitate fluid flow resulting in improved performance [1]. The hindrance of hydrocarbon flow by faults is due to very low permeability and high entry pressure compared to reservoir rock. This paper

presents simulation sensitivity studies on fluid conductivity in a fault characterised by different permeability, entry pressure and thickness.

EXPERIMENTAL WORK

The experimental work involved determination of fluid and rock properties to select representative material for the fault zone - **Table 1**. Mercury intrusion porosimetry was conducted on ceramic material to represent the fault zone and on Berea sandstone as the reservoir rock to establish simulation parameters. The oil breakthrough determined by the experimental set up in **Fig. 1** was used as a control to the modeling sensitivity studies.

SIMULATION STUDIES

Description of the simulation models: The models are two-phase oil and water with simplified 1D geometry. They are composite and consist of reservoir and fault zones with aggregate dimensions of 5.92 cm by 3.8 cm and 200x1 Cartesian grid blocks in the x- and y-directions respectively. The blocks have uniform sizes with center-point geometry. A simplified reservoir model with two compartments is shown in **Fig. 3** but only zone A has been considered. **Table 2** shows the simulated models at laboratory conditions.

Reservoir zone: This zone is 4.93 cm by 3.8 cm and has 150x1 blocks. Three conditions were modeled by varying initial water saturation. Case 1: S_w=1 - represents oil migration when oil is the injected phase. Case 2: S_w=S_{wi} (no movable water) - represents a reservoir model located high on a S_w-log. Case 3: 1>S_w>S_{wi} (contains movable water, 20% PV) - represents a model located lower on a S_w-log. Intermediate wettability was assumed.

Fault zone: The zone is 0.99 cm by 3.8 cm and has 50x1 blocks initially saturated 100% with water. The damage zone phenomenon often encountered in faults was ignored and a uniform rock was assumed [4]. The fault is characterised by very low permeability and high oil entry pressure. The measured permeability is 0.00295 md but models with permeability of 0.000295 or 0.0295 md were also simulated. Also, the measured entry pressure is 8 bar but other models with entry pressures of 4 and 14 bar were simulated - **Table 2**.

Relative permeability and capillary pressure: Relative permeability and capillary pressure data (**Fig. 2**) for the two zones were generated from Corey correlations using the measured rock parameters [5.]. Oil flow across the fault can only occur after establishing a differential pressure greater than the capillary forces; achieved by pressure drawdown due to production or by buoyancy from the oil column. However, pressure due to buoyancy forces in small-scale models may be negligible to force oil into the fault pores. Here, differential pressure was achieved by drawdown due to production from the fault zone.

Production/injection controls: Two vertical wells - a producer and an injector were defined in the models - **Fig. 3**. The producer was located in the last grid block (200,1) at the edge of the fault zone while the injector was located in the first grid block (1,1) in the reservoir zone. Production was

controlled by bottom hole pressure and the minimum pressure in the producer was set to atmospheric pressure. Injection was controlled by constant pressure of 18 bar. Production time was limited to 500 hours.

RESULTS AND DISCUSSIONS

The simulation results are shown in **Figs. 4** to **17** and the discussion is mainly related to properties of the fault zone. **Figs. 4** and **5** show water saturation in the composite model after oil breakthrough; indicating high oil build-up at the Berea/ceramic interface. The breakthrough delayed after the fault entry pressure was exceeded because the oil saturation had to exceed the critical saturation to enhance mobility in the fault zone.

The breakthrough and subsequent recoveries also depend on the fault thickness as shown in **Fig. 6**. It should be noted that the recovered oil is higher than the pore volume of the Berea sample because of continued oil injection. When the fault thickness was ten times the measured value the breakthrough delayed by over ten times while it was much earlier when the fault thickness was reduced by a factor of ten. This shows that fault thickness can affect performance of a compartmentalised reservoir and may experience abrupt increase in oil recovery in its lifetime or continuous decline, depending on well location.

The influence of varying fault permeability on oil recovery is shown in **Figs. 7** and **8** where the entry pressure and thickness were kept constant at the measured values. As expected the breakthrough is much earlier in the model with highest permeability and the corresponding oil recovery is highest. This is because the entry pressure was exceeded much earlier due to a faster drawdown - **Fig. 9**. The results clearly show that tight faults affect oil migration and can significantly influence the performance of compartmentalised reservoirs.

The variation in the fault entry pressure on reservoir performance is summarised in **Figs. 10** and **11** where early oil breakthrough and high recoveries were observed in models with lower entry pressures. A combination of entry pressure and permeability shows that the performance is controlled more by variation in permeability rather than entry pressure. However, this could also be due to the narrow variation in the entry pressure compared to the variation in permeability. The entry pressure is a key rock parameter and can be predicted from NMR capillary pressure curves [6]. It is essential when it comes to problems such as predicting the strength of sealing rocks or understanding transitional zones.

The pressure profiles in the fault zone in **Figs. 12** to **16** show shorter transient periods and early steady-state water flow in models with high permeability and low entry pressure. This is expected and is also reflected by the early oil breakthrough. **Fig. 16** shows pressure profiles before/after oil breakthrough; indicating virtual steady-state oil flow in the fault zone at later stages of production when the water flow has apparently ceased.

Fig. 17 shows that the oil breakthrough and recovery can also depend on initial saturation conditions in the reservoir zone. This, however, has more to do with fluid flow properties in the reservoir zone rather than properties of the fault. A vertical fault was assumed in this work but other factors neglected like fault orientation and dead zones may also influence reservoir performance [4]. A comparison of the experimental and simulation results in **Table 2** shows more or less the same breakthrough periods, but proper procedure requires that such results are up-scaled to field conditions before final interpretation and application.

CONCLUSIONS

The simulations have shown that oil breakthrough and recovery across fault zones in compartmentalised reservoirs are controlled by the interplay of fault rock properties (i.e. entry pressure, permeability and thickness) and fluid properties.

REFERENCES

1. Aydin, A.: "Fractures, Faults, and Hydrocarbon Entrapment, Migration and Flow," *Marine and Petroleum Geology*, **Vol. 18** (2001) pp. 1063-1081.
2. Flodin, E.A., Aydin, A., Durlofsky, L.J., and Yeten, B.: "Representation of Fault Zone Permeability in Reservoir Flow Models," SPE 71617, *Annual Technical Conference and Exhibition*, New Orleans, Louisiana (30 Sept.-3 Oct. 2001).
3. Fisher, Q.J., and Knipe, R.J.: "The Permeability of Faults Within Siliciclastic Petroleum Reservoirs of the North Sea and Norwegian Continental Shelf," *Marine and Petroleum Geology*, **Vol. 17** (2000) 1794-814
4. Fisher, Q.J., Harris, S.D., McAllister, E., Knipe, R.J., and Bolton, A.J.: "Hydrocarbon Flow Across Faults by Capillary Leakage Revisited," *Marine and Petroleum Geology*, **Vol. 18** (2001) pp. 251-257.
5. Brooks, R.H., and Corey, A.T.: "Properties of Porous Media Affecting Fluid Flow," *J. of the Irrigation and Drainage Division, Proc. of ASCE* (1966), **Vol. 92**, No. IR2, pp 61-88.
6. Volokitin, Y., Looyestijn, W.J., Slijkerman. W.F.J., and Hofman, J.P.: "A Practical Approach to Obtain 1st Drainage Capillary Pressure Curves from NMR Core and Log Data," *SCA-9924, Int. Symp. of the Society of Core Analysts*, Colorado School of Mines Golden, Colorado, USA (Aug. 1-4, 1999).

NOMENCLATURE

k = permeability, md
Pe = capillary entry pressure, bar
S_w = water saturation
t = time, hour
t_BT = breakthrough - Table 2 & Figs. 12-15
ABT = after breakthrough - Fig. 15
BBT = before breakthrough - Fig. 15
FOPT = field oil production total, scc
L = fault thickness, cm
PV = pore volume, cc
WWCT = well water cut
ϕ = porosity
μ = viscosity, cp
λ = pore size distribution index
ρ = density, kg/m^3
σ = surface tension, mN/m
Subscripts: o=oil, w=water, i=irreducible

Table 1? Measured rock and fluid properties.

Core	Material type	Function	S_{wi}	L, cm	f	k, md	l	Pe, bar
Ceramic	artificial compound	fault	0.2	1.06	0.3	0.00295	2	8.0
Berea	sandstone	reservoir	0.1	4.93	0.23	230	1.15	0.05
Chalk	chalk	fault	0.2-0.3	1.0-5.0	0.2-0.4	~ 3	2.9	1.1

Fluid properties			
Water density, ?$_w$ (kg/m^3)	1027	water viscosity, μ_w (cp)	1.0
Oil (Exxol-D60) density, ?$_o$ (kg/m^3)	790	oil viscosity, μ_o (cp)	1.28
Surface tension, s (mN/m)	37.0	salinity, g/l	26.7

Table 2?Simulated cases: The rock properties are represented as: k1=0.0295 md, k2=0.00295 md, k3=0.000295 md, Pe1=4 bar, Pe2=8 bar, Pe3=14 bar, L1=0.099 cm, L2=0.99 cm and L3=9.9 cm.

Model	Reservoir zone	Fault zone				Injected phase	T_BT, hours	
	S_w	S_w	k (md)	Pe (bar)	L (cm)		Simulation	Experiment
M1	1.0	1.0	0.0295	8.0	0.99	oil	12	
M2	1.0	1.0	0.00295	8.0	0.99	oil	14	13
M3	1.0	1.0	0.000295	8.0	0.99	oil	15	
M4	1.0	1.0	0.00295	8.0	0.099	oil	5	
M5	1.0	1.0	0.00295	8.0	9.9	oil	232	
M6	1.0	1.0	0.00295	4.0	0.99	oil	14	
M7	1.0	1.0	0.00295	14.0	0.99	oil	16	
M8	1.0	1.0	0.000295	4.0	0.99	oil	140	
M9	1.0	1.0	0.000295	8.0	0.99	oil	145	
M10	1.0	1.0	0.000295	14	0.99	oil	160	
M11	0.1	1.0	0.00295	8.0	0.99	Oil	8	6
M12	0.3	1.0	0.00295	8.0	0.99	oil/water	10	9

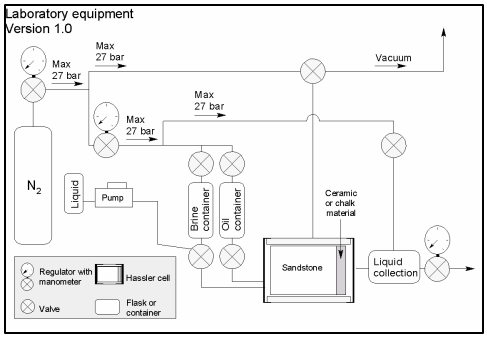

Fig. 1? Expeimental set up.

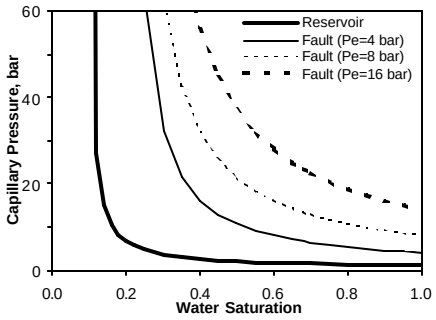

Fig. 2? Capillary pressure curves.

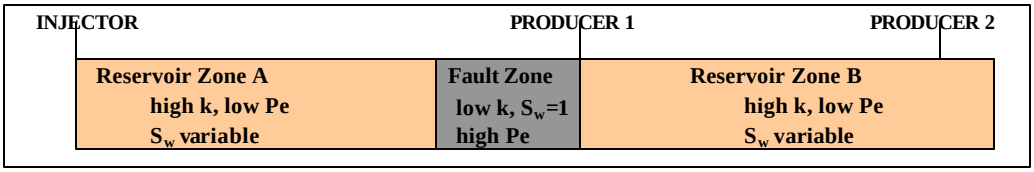

Fig. 3? Overviw of a compartmentalised reservoir model.

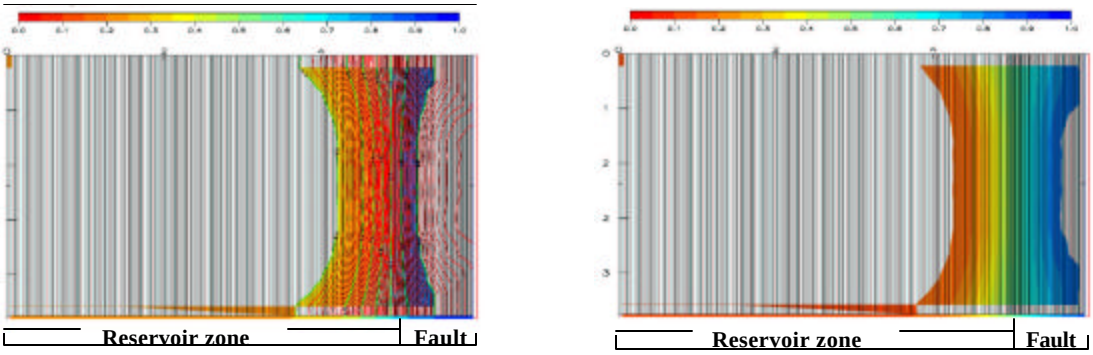

Fig. 4? Water saturation: contour plot.

Fig. 5? Water saturation: later time step.

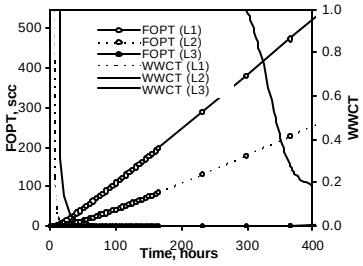

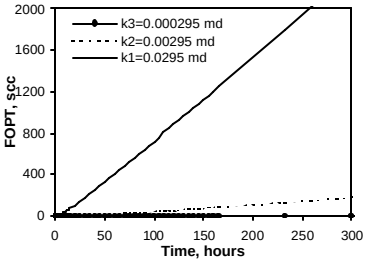

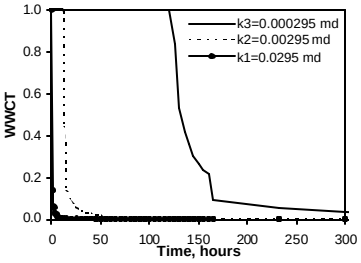

Fig. 6? Oil recovery and water cut.

Fig. 7? Oil recovery: Pe=8 bar.

Fig. 8? Water cut: Pe=8 bar.

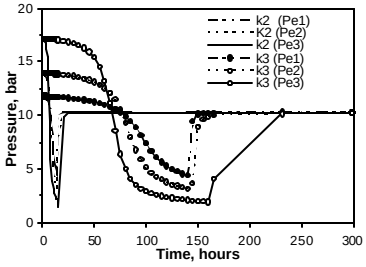

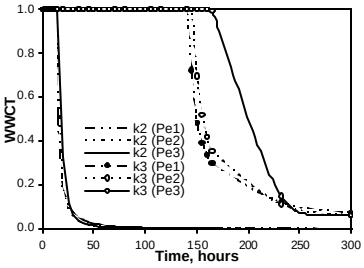

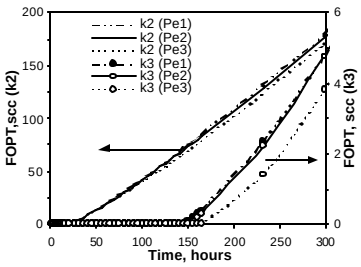

Fig. 9? Pressure drawdown.

Fig. 10? Well water cut.

Fig. 11? Oil recovery.

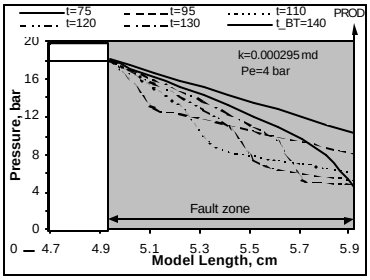

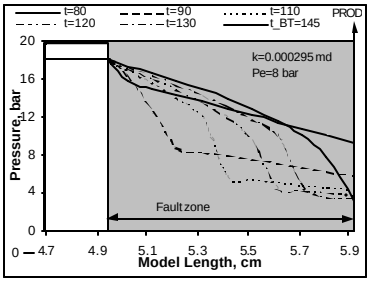

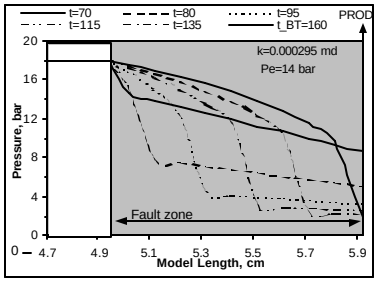

Fig. 12? Fault pressure: M8.

Fig. 13? Fault pressure: M9.

Fig. 14? Fault pressure: M10.

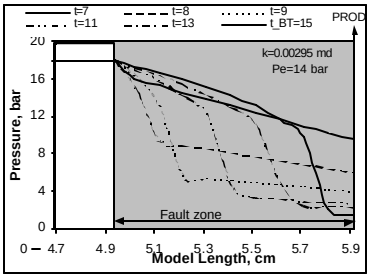

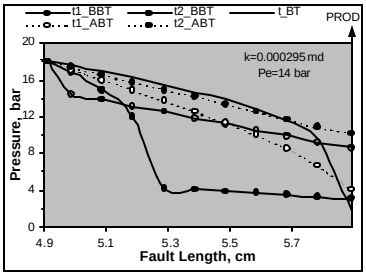

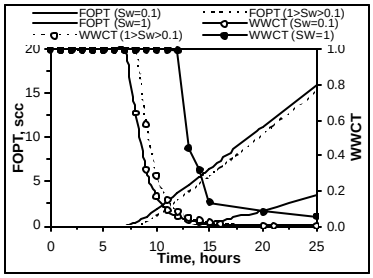

Fig. 14? Fault pressure: M7.

Fig. 15? Fault pressure: M10.

Fig. 16? Water cut and oil recovery